

Effect of Thermal Treatment on the Thermoelectric Properties of $\text{Sb}_{0.9}\text{Bi}_{1.1}\text{Te}_{2.9}\text{Se}_{0.1}$ Solid Solution Thin Films

Y. E. Kalinin*, V. A. Makagonov, and A. V. Sitnikov

Voronezh State Technical University, Voronezh, 394026 Russia

*e-mail: kalinin48@mail.ru

Abstract—The effect thermal treatment in a vacuum has on the thermoelectric properties of $\text{Sb}_{0.9}\text{Bi}_{1.1}\text{Te}_{2.9}\text{Se}_{0.1}$ solid solution thin films obtained via ion-beam sputtering in an argon atmosphere is considered. It is established that the specific resistance and thermopower are determined by the type and concentration of intrinsic point defects of the $\text{Sb}_{0.9}\text{Bi}_{1.1}\text{Te}_{2.9}\text{Se}_{0.1}$ solid solution. The power factor values are found to be comparable to those of nanostructured materials based on $(\text{Bi,Sb})_2(\text{Te,Se})_3$ solid solutions.

DOI: 10.3103/S1062873816090227

In this work, we present the results from investigating the effect thermal treatment has on the structure and thermoelectric properties of thin nanostructured films of $\text{Sb}_{0.9}\text{Bi}_{1.1}\text{Te}_{2.9}\text{Se}_{0.1}$ solid solutions obtained via ion-beam sputtering on a ceramic target and the subsequent deposition of the material onto a glassceramic substrate [1]. The thickness of the obtained films was measured on a MII-4 interferometer and varied within 2.5 and 3 μm .

The structure was investigated by means of X-ray diffraction on a Bruker D2 Phaser diffractometer, and the results were processed with the Bruker DIFFRAC EVA 3.0 and TOPAS 4.2 software packages. The thermopower dependences were measured at room temperature using the hot probe technique. A silver wire of 99.999% purity served as the material of our cold and hot probes.

The specific resistance dependences were measured according to the two-probe technique with a direct current using a V7-78/1 universal digital multimeter. The relative error in measuring the electric resistance did not exceed 2%, while that of measuring the thermopower did not exceed 3% for the studied samples. Thermal treatment and measurements of the temperature dependences of the specific resistance were performed in a vacuum at a residual gas pressure of no more than 5×10^{-5} Torr. The temperature increase and cooling rates were 2 to 3 deg min^{-1} . The thermally treated samples were held at annealing temperatures for 60 min.

The temperature dependence of the specific resistance for our $\text{Sb}_{0.9}\text{Bi}_{1.1}\text{Te}_{2.9}\text{Se}_{0.1}$ thin-film solid solution is shown in Fig. 1. In the $\rho(T)$ dependence for heating, there are two kinks at $T_1 = 50^\circ\text{C}$ and $T_2 = 150^\circ\text{C}$, after each of which a region of a sharper change

in the electric resistance with rising temperature is observed (curve 1). With a falling temperature (curve 2), the specific resistance grows monotonically, evidence of retention of a semiconductor-conductivity type and no reversible structure changes.

To determine exactly how thermal treatment affects the structure and thermoelectric properties of $\text{Sb}_{0.9}\text{Bi}_{1.1}\text{Te}_{2.9}\text{Se}_{0.1}$ solid solution, a series of annealing experiments was performed at different temperatures in a vacuum. The structure, thermopower, and the specific resistance were investigated for all samples.

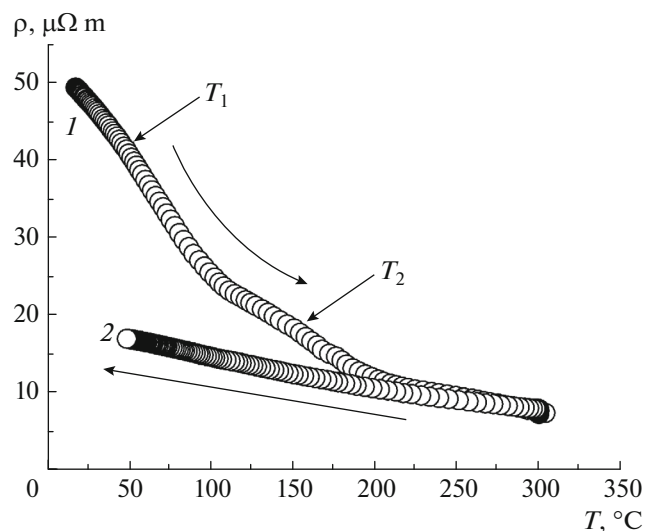


Fig. 1. Temperature dependences of specific resistance for our $\text{Sb}_{0.9}\text{Bi}_{1.1}\text{Te}_{2.9}\text{Se}_{0.1}$ thin-film solid solution, obtained upon heating (curve 1) and cooling (curve 2).

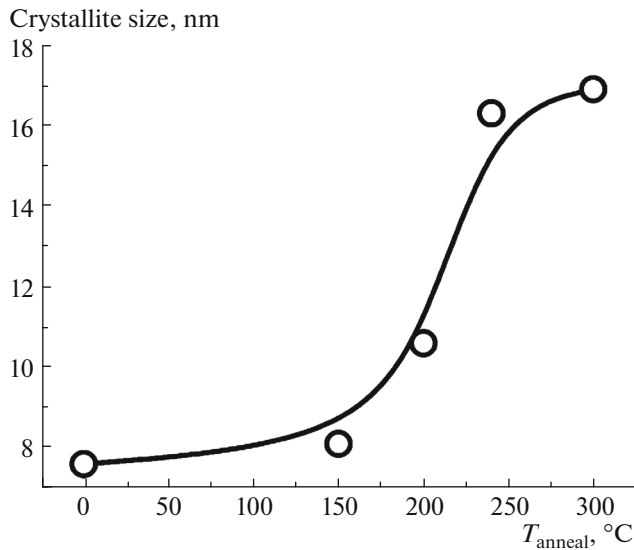


Fig. 2. Dependences of the crystallite size for our $\text{Sb}_{0.9}\text{Bi}_{1.1}\text{Te}_{2.9}\text{Se}_{0.1}$ solid solution on the temperature of annealing in a vacuum for 60 min. The point at 0°C corresponds to the crystallite size in the initial state.

To estimate the contribution from recrystallization processes to the drop in electrical resistance, the crystallite size of the $\text{Sb}_{0.9}\text{Bi}_{1.1}\text{Te}_{2.9}\text{Se}_{0.1}$ thin film was measured with respect to annealing temperature (Fig. 2). After treatment at 150°C, the process of active collective recrystallization commenced, and was accompanied by a quick doubling of crystallite sizes. Raising the temperature of treatment above 240°C slowed the recrystallization, indicating that the structure of such films is closer to the equilibrium state. The recrystallization process that begins at $T_2 = 150^\circ\text{C}$ (Fig. 2) reduced the proportion of grain boundaries with high electrical resistance and to a corresponding drop in the specific resistance of the obtained films (Fig. 1). The specific resistance in the region of 150–250°C was more than halved.

The effect 60 min of thermal treatment had on the thermopower and specific resistance of our $\text{Sb}_{0.9}\text{Bi}_{1.1}\text{Te}_{2.9}\text{Se}_{0.1}$ thin films measured at room temperature is shown in Fig. 3. The dependence of specific resistance on the annealing temperature is nonmonotonic with a minimum observed at an annealing temperature of $T_{\text{anneal}} = 190^\circ\text{C}$. On the dependence of the thermopower of our $\text{Sb}_{0.9}\text{Bi}_{1.1}\text{Te}_{2.9}\text{Se}_{0.1}$ thin films on the annealing temperature, the sign changes from negative to positive at $T_{\text{anneal}} = 190^\circ\text{C}$, evidence that the dominant type of charge carrier changes from negatively charged electrons to positive holes.

The dependence of power factor $PF = \alpha^2/\rho$ on the annealing temperature is of special interest. Like the dependence of the specific resistance on the annealing temperature, it is nonmonotonic. When the annealing

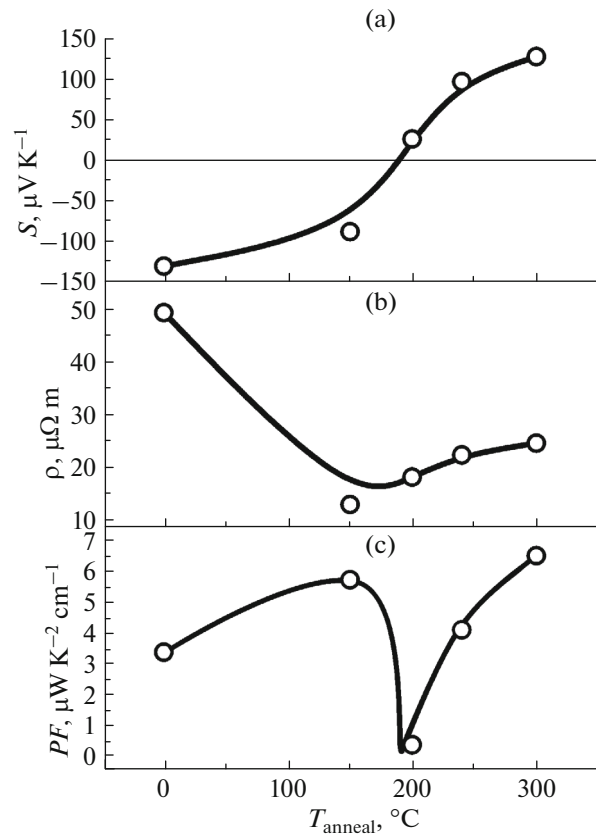


Fig. 3. (a) Thermopower, (b) specific resistance, and (c) power factor for our $\text{Sb}_{0.9}\text{Bi}_{1.1}\text{Te}_{2.9}\text{Se}_{0.1}$ thin films vs. the temperature of annealing in a vacuum for 60 min. The points at 0°C correspond to the sample's properties in the initial state.

temperature is raised to 150°C, the power factor grows in proportion to the drop in the specific resistance, since the thermopower falls slightly (by ~20%) in this temperature range. The power factor then falls to zero at $T_{\text{anneal}} = 190^\circ\text{C}$ in the region of the change in the sign of the thermopower. A further rise in the annealing temperature leads to a small increase in the specific resistance; however, a strong increase in the absolute thermopower results in a sharp rise in the power factor. A remarkable feature of these results is that for the samples annealed at 150 and 300°C, thermal treatment alone allowed us to obtain materials with the same elemental composition but with differing types of conductivity and apparently the same power factors. At the same time, the absolute values of the power factor are comparable to those for nanostructured bulk materials based on $(\text{Bi,Sb})_2(\text{Te,Se})_3$ solid solutions [2].

The change in the sign of the thermopower and the nonmonotonic dependence of the specific resistance on the annealing temperature for $\text{Sb}_{0.9}\text{Bi}_{1.1}\text{Te}_{2.9}\text{Se}_{0.1}$ solid solution thin films could result from the existence of nonequilibrium point defects (antisite defects

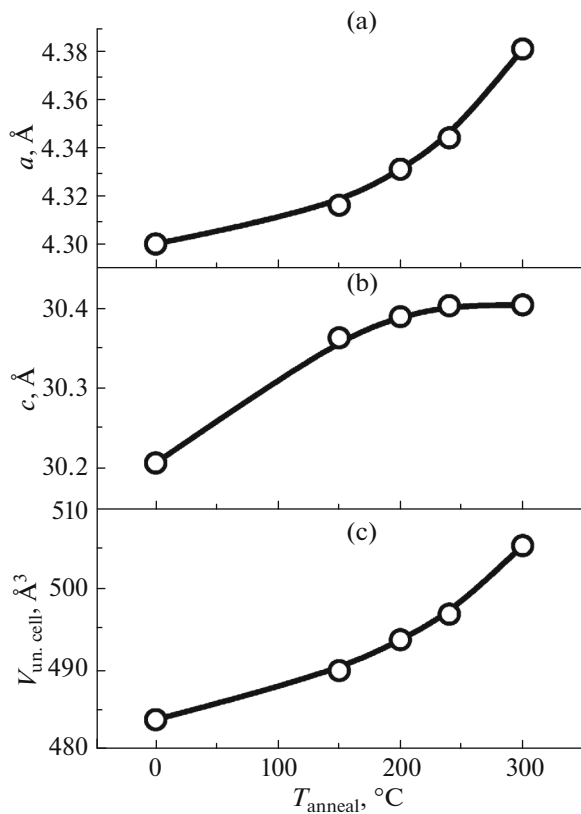


Fig. 4. Dependences of lattice parameters (a) a and (b) c and (c) the crystal lattice unit cell volume for our $\text{Sb}_{0.9}\text{Bi}_{1.1}\text{Te}_{2.9}\text{Se}_{0.1}$ thin films on the temperature of thermal treatment in a vacuum for 60 min.

and vacancies). There could also be pairs of point defects, e.g., pairs of antisite defects of metal and chalcogen [3, 4].

It is well known that solid solutions based on $(\text{Bi,Sb})_2(\text{Te,Se})_3$ typically contain intrinsic point defects (IPDs) that emerge even in stoichiometric compositions [5, 6]. As they do, such negatively charged antisite defects as Bi_{Te}^- , Sb_{Te}^- , and Bi_{Se}^- , formed when excess cations occupy lattice vacancies in the anionic sublattice, are acceptor-type defects [7], while positively charged anionic vacancies (V_{Te}^{2+} and V_{Se}^{2+}) are donor-type defects [8].

To clarify the nature of the defects that emerge during ion-beam sputtering, and to study the effect

Crystal lattice parameters (a and c) of the $\text{Sb}_1\text{Bi}_1\text{Te}_3$ solid solution, according to different literature sources

a , Å	c , Å	Source
4.328	30.476	[9]
4.326	30.488	[10]
4.33	30.50	[11]

thermal treatment has on them, we investigated the dependence of the crystal lattice parameters for our $\text{Sb}_{0.9}\text{Bi}_{1.1}\text{Te}_{2.9}\text{Se}_{0.1}$ solid solution on the annealing temperature (Fig. 4). For comparison, the lattice parameters (a and c) given by different literature sources for the $\text{Sb}_1\text{Bi}_1\text{Te}_3$ solid solution are presented in the table. Analysis of the data in Fig. 4 and the table showed that the lattice parameters of the $\text{Sb}_{0.9}\text{Bi}_{1.1}\text{Te}_{2.9}\text{Se}_{0.1}$ for thin films obtained via ion-beam sputtering were lower than those specified in the reference literature.

According to [12], the sizes of atoms in the $\text{Sb}_{0.9}\text{Bi}_{1.1}\text{Te}_{2.9}\text{Se}_{0.1}$ solid solution are $\text{Bi} = 0.17$ nm, $\text{Sb} = 0.159$ nm, $\text{Te} = 0.16$ nm, and $\text{Se} = 0.14$ nm. Since the atomic radii of Sb and Te are approximately the same, and the Se content in the obtained thin films is much lower than that of Te, the lower values of a and c lattice parameters (as compared to the literature) could be due to the presence of vacancy-type defects in the crystal lattice. As the annealing temperature rises, lattice parameters a and c of the $\text{Sb}_{0.9}\text{Bi}_{1.1}\text{Te}_{2.9}\text{Se}_{0.1}$ thin films grow monotonically, reaching the reference data for the $\text{Sb}_1\text{Bi}_1\text{Te}_3$ solid solution at $T_{\text{anneal}} = 300^\circ\text{C}$ (parameter a even grows a bit more). Therefore, either interstitial-type defects or antisite defects appear upon an increase in the annealing temperature.

Combined analysis of the results of measurements of crystal lattice parameters of the $\text{Sb}_{0.9}\text{Bi}_{1.1}\text{Te}_{2.9}\text{Se}_{0.1}$ thin films and thermoelectric properties indicates that the main type of point defects formed in the grain bulk during ion-beam sputtering are vacancy-type IPDs. During thermal treatment, the number of nonequilibrium donor defects (V_{Te}^{2+} and V_{Se}^{2+} vacancies) falls and the number of acceptor defects (Bi_{Te}^- and Sb_{Te}^- antisite defects) rises, accompanied by changes in the material's thermoelectric properties.

CONCLUSIONS

The increase in electrical conductance upon raising the temperature of the thermal treatment of $\text{Sb}_{0.9}\text{Bi}_{1.1}\text{Te}_{2.9}\text{Se}_{0.1}$ thin-film samples to $T_{\text{anneal}} = 190^\circ\text{C}$ is a result of a reduction in the number of grain boundaries with high contact resistance and the annealing of nonequilibrium donor vacancy-type IPDs, leading to a drop in concentration and a simultaneous increase in the mobility of electrons. The number of acceptor defects (Bi_{Te}^- and Sb_{Te}^- antisite defects) rises concurrently, compensating for the donors, and is reflected in the lower absolute thermopower at $T_{\text{anneal}} < 190^\circ\text{C}$. Upon annealing at $T_{\text{anneal}} > 190^\circ\text{C}$, the number of grain boundaries falls as well, and even much more sharply than when $T_{\text{anneal}} < 190^\circ\text{C}$. Nevertheless, the number of acceptor defects rises, accompanied by the type of dominant charge carriers changing to holes. The simultaneous increase in the specific resistance when the annealing temperature is raised above 190°C

is evidence that hole mobility falls as the number of antisite defects rises, and the rise in absolute thermopower indicates that the degree of compensation of the semiconductor (which is now of the acceptor type) is reduced.

ACKNOWLEDGMENTS

This work was supported by the RF Ministry of Education and Science as part of a Federal Target Program (agreement no. 14.577.21.0202, unique identifier RFMEFI57715X0202).

REFERENCES

1. Kalinin, Yu.E., Makagonov, V.A., and Sitnikov, A.V., *Phys. Solid State*, 2015, vol. 57, no. 10, p. 1953.
2. Poudel, B., Hao, Q., Ma, Y., et al., *Science*, 2008, vol. 320, no. 5876, p. 634.
3. Gerovac, N., Snyder, G.J., and Caillat, T., *Proc. 21st Int. Conf. on Thermoelectrics*, Long Beach, CA, 2002, pp. 31–34.
4. Kim, H.-C., Lee, J.-S., Oh, T.-S., et al., *Proc. 17th Int. Conf. on Thermoelectrics*, Nagoya, 1998, pp. 125–128.
5. Gol'tsman, B.M., Kudinov, V.A., and Smirnov, I.A., *Poluprovodnikovye termoelektricheskie materialy na osnove Bi_2Te_3* (Semiconductor Thermoelectric Materials Based on Bi_2Te_3), Moscow: Nauka, 1972.
6. Hu, L., Zhu, T., Liu, X., et al., *Adv. Funct. Mater.*, 2014, vol. 24, no. 33, p. 5211.
7. Stary, Z., Horak, J., Stordeur, M., et al., *J. Phys. Chem. Solids*, 1988, vol. 49, p. 29.
8. Horak, J., Stary, Z., Lostak, P., et al., *J. Phys. Chem. Solids*, 1990, vol. 51, p. 1353.
9. Smith, M.J., Knight, R.J., and Spencer, C.W., *J. Appl. Phys.*, 1962, vol. 33, p. 2186.
10. Becebrede, W.R. and Guentert, O.J., *J. Phys. Chem. Solids*, 1962, vol. 23, p. 1023.
11. Stasova, M.M. and Abrikosov, N.Kh., *Izv. Akad. Nauk SSSR, Neorg. Mater.*, 1970, vol. 6, p. 1090.
12. Richoux, V., Diliberto, S., and Boulanger, C., *J. Electron. Mater.*, 2010, vol. 39, p. 1914.

Translated by Z. Smirnova